Fermi surface of the colossal magnetoresistance perovskite $La_{0.7}Sr_{0.3}MnO_3$

1999 J. Phys.: Condens. Matter 11 L279

(http://iopscience.iop.org/0953-8984/11/25/104)

J. Phys.: Condens. Matter **11** (1999) L279–L285. Printed in the UK PII: S0953-8984(99)04210-1

LETTER TO THE EDITOR

Fermi surface of the colossal magnetoresistance perovskite $La_{0.7}Sr_{0.3}MnO_3$

E A Livesay†, R N West†, S B Dugdale‡§, G Santi§ and T Jarlborg§

† Physics Department, University of Texas at Arlington, Arlington, PO Box 19059, Texas, TX 76019, USA
‡ H H Wills Physics Laboratory, University of Bristol, Tyndall Avenue, Bristol BS8 1TL, UK
§ Département de Physique de la Matière Condensée, Université de Genève, 24 quai Ernest Ansermet, CH-1211 Genève 4, Switzerland

Received 11 May 1999

Abstract. Materials that exhibit colossal magnetoresistance (CMR) are currently the focus of an intense research effort, driven by the technological applications that their properties suggest. Using the angular correlation of photons from electron–positron annihilation, we present a first view of the Fermi surface of a material that exhibits CMR, supported by 'virtual crystal' electronic structure calculations. The Fermi surface is shown to be sufficiently cubic in nature that it is likely to support nesting.

Since the recent discovery of the phenomenon of colossal magnetoresistance (CMR), research efforts have been intense [1–3]. The reason is the number of potentially important applications for CMR materials in magnetic memory systems, magnetic read heads and in other sensors [4]. Experimental studies of CMR materials have concentrated on the manganite perovskites [3], $T_{1-x}D_xMnO_3$, where T is a trivalent lanthanide cation and D is a divalent (e.g. alkaline earth) cation. As implied by the Jahn–Teller distortions manifest in the undoped parent compound $LaMnO_3$, these are systems where there is strong coupling between the electronic and lattice degrees of freedom [5]. That, and the multiplicity of crystallographic and magnetic phases in the doped crystals, suggests that the ground states of these systems depend upon a subtle interplay between their microscopic electrical, magnetic and lattice properties and excitations [6, 7]. Calculations of electronic band structures have been reported [7, 8], but experimental evidence concerning those band structures and their associated electronic spectra remains scarce.

In particular, a knowledge of the Fermi surface (FS) is vital for an understanding of transport properties. The nearly half-metallic character (the existence of a significant FS in only one spin) of these materials is clearly of importance, because of its implications with respect to a spin-flip scattering contribution to the resistivity. Moreover, there has been speculation that one of the FS sheets has nesting properties [9], implying additional consequences for the transport. In this letter, we present the first clear-cut experimental evidence of the major FS sheet of $La_{0.7}Sr_{0.3}MnO_3$ which is in close agreement with our calculations of the momentum density and band structure.

In such complicated systems, the traditional magneto-oscillatory tools of fermiology are precluded, since the disordered nature of the alloy means that the electronic mean-free-paths are too short. However, the occupied momentum states, and hence the FS, can be accessed

0953-8984/99/250279+07$19.50

via the momentum distribution using the two-dimensional angular correlation of electron–positron annihilation radiation (2D-ACAR) technique [10]. A 2D-ACAR measurement yields a 2D projection (integration over one dimension) of an underlying two-photon momentum density, $\rho(\boldsymbol{p})$.

$$\rho(\boldsymbol{p}) = \sum_{occ\cdot j,\boldsymbol{k}} \left| \int \mathrm{d}\boldsymbol{r} \sqrt{\gamma(\boldsymbol{r})}\psi_{k,j}(\boldsymbol{r})\psi_{+}(\boldsymbol{r}) \exp(-\mathrm{i}\boldsymbol{p}\cdot\boldsymbol{r}) \right|^2 = \sum_{j,\boldsymbol{k},\boldsymbol{G}} n^j(\boldsymbol{k}) |C_{\boldsymbol{G},j}(\boldsymbol{k})|^2 \delta(\boldsymbol{p} - \boldsymbol{k} - \boldsymbol{G}) \quad (1)$$

where $\psi_{k,j}(\boldsymbol{r})$ and $\psi_{+}(\boldsymbol{r})$ are the electron and positron wave functions, respectively, $n^j(\boldsymbol{k})$ is the electron occupation density in $\boldsymbol{k}$-space in the jth band, and $\gamma(\boldsymbol{r})$ is a so-called enhancement factor which takes account of electron–positron correlations (it would be unity in the independent particle model) [11]. The $C_{G,j}(\boldsymbol{k})$ are the Fourier coefficients of the enhanced electron–positron wave function product and the delta function expresses the conservation of crystal momentum, $\boldsymbol{p} = \hbar(\boldsymbol{k} + G)$. $\rho(\boldsymbol{p})$ is a single-centred distribution having the full point symmetry of the the crystal lattice in question and of a form determined by the nature of the annihilated states. In a metal, it contains, in addition, discontinuities at various points $\boldsymbol{p}_F = \hbar(\boldsymbol{k}_F + \boldsymbol{G})$ throughout the momentum density which reflect the FS. When that FS is the matter of paramount interest the Lock–Crisp–West procedure [12] is often followed. Here the various FS discontinuities are superimposed by folding $\rho(\boldsymbol{p})$ (or its measured projections) back into the first Brillouin zone (BZ). The result is a new $\boldsymbol{k}$-space density, $\sum_{j,\boldsymbol{k}} n^j(\boldsymbol{k}) \sum_{\boldsymbol{G}} |C_{\boldsymbol{G},j}(\boldsymbol{k})|^2$, which aside from the factor $\sum_{\boldsymbol{G}} |C_{\boldsymbol{G},j}(\boldsymbol{k})|^2$ (usually a weak function of $\boldsymbol{k}$ within each band) is simply the electron occupation density.

The $La_{0.7}Sr_{0.3}MnO_3$ sample was cut with a diamond saw from a cylinder grown using the floating-zone technique by the group of Tokura [13]. The specimen was then mechanically polished. Although the structure of $La_{0.7}Sr_{0.3}MnO_3$ is distorted from the ideal perovskite, the theoretical calculations and the treatment of the experimental data were made, for simplicity, under the assumption of an undistorted cubic perovskite. The sample was aligned using Laue x-ray back-reflection to ensure that the projection direction would be down the crystalline [001] axis. The experimental spectra were measured on the UTA 2D-ACAR spectrometer [14] at a temperature of ∼30 K. The FWHM of the total experimental resolution, which is well described by a Gaussian, was of the order of 11% of the size of the BZ. A total of ∼400 million counts were accumulated. After verification that the spectrum exhibited the appropriate symmetry, that symmetry was then forced upon it by folding, thereby increasing the effective number of counts to more than 3×10^9.

The spin-dependent momentum densities were calculated using the linearized muffin-tin orbital (LMTO) method within the atomic sphere approximation (ASA), including combined-correction terms [15]. The exchange-correlation part of the potential was described, in separate calculations, in both the local spin-density (LSDA) and generalized-gradient approximations (GGA, [16]), but there was no significant difference in the results obtained. Consequently, those presented here use the LSDA. The self-consistent band-structure was calculated at 364 k-points in the irreducible 1/48th part of the BZ using a basis set of s, p and d functions. The lattice parameter was set to a value of 3.89 Å, obtained from a linear interpolation of the experimental values from other Sr compositions [13]. The electronic wave functions were then used to generate the electron momentum densities for the up- and down-spin bands separately. In the construction of the momentum density, 2095 reciprocal lattice vectors were used. A full description of the technique is given in the papers of Andersen [15] and Singh and Jarlborg [17]. To simulate the Sr^{2+} doping, a 'virtual crystal' approach was employed, whereby the self-consistency was realised in a cell with the La^{3+} ions replaced by virtual '2.7+'

ions (i.e. with 2.7 protons). While being a relatively vulgar way of describing the doping, our calculations and those of others (for example, see [8,9]), have shown it to explain the systematic trends in the electronic structure. The calculated momentum distributions were numerically integrated (along the [001] direction) for direct comparison with the experiment.

In figure 1, the band structure along the usual high-symmetry directions is plotted. The bands are similar to those calculated by Pickett and Singh [9] and Youn and Min [8]. The Fermi level lies just above a gap in the minority density-of-states, indicating that the system is very close to being half-metallic. At the Fermi level, the bands have mainly Mn d character (these are the e_g bands; the t_{2g} bands are the more localized set of bands, lying a couple of eV below the Fermi energy). However, it can be seen that there are two small minority electron sheets; a tiny downward shift in the Fermi energy would make these disappear, the system becoming half-metallic.

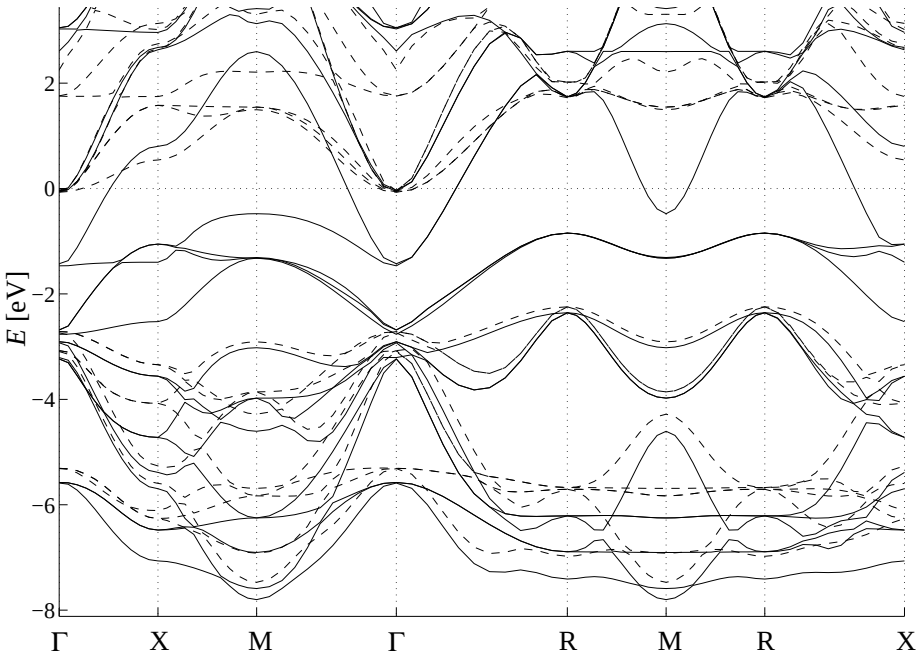

Figure 1. Spin-polarized band structure of $La_{0.7}Sr_{0.3}MnO_3$. The majority bands are shown as solid lines, and the minority as dashed lines. Note that the Fermi energy lies just above a gap in the minority bands.

Figure 2 shows the two principal majority FS sheets coming from the LMTO calculation. These comprise hole cuboids at the *R* points (coined 'woolsacks') that touch an electron spheroid centred at the Γ point along the ⟨111⟩ directions. These woolsacks, with their relatively flat faces, present the possibility of carrier 'skipping' along the parallel sections of surface (with the initial and final velocities remaining parallel), in addition to supporting a FS capable of nesting [9]. Both of these have implications for the transport properties owing to the concentration of phase-space for the scattering along directions parallel to the cube edges, as noted by Pickett *et al* for the flat, quasi-one-dimensional parts of the FS of the cuprates [18]. Clearly, the degree of flatness of the sides of these 'woolsacks' will determine the strength of these nesting and skipping tendancies; we will return to this later when we discuss the experimental results.

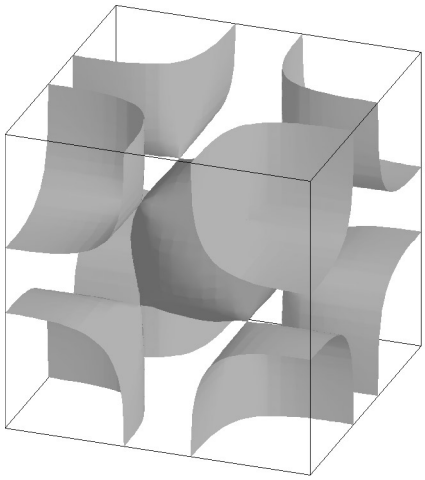

Figure 2. Two sheets of the Fermi surface of $La_{0.7}Sr_{0.3}MnO_3$. Hole cuboids at the *R* points, coined 'woolsacks'. Electron spheroid centred at the Γ point.

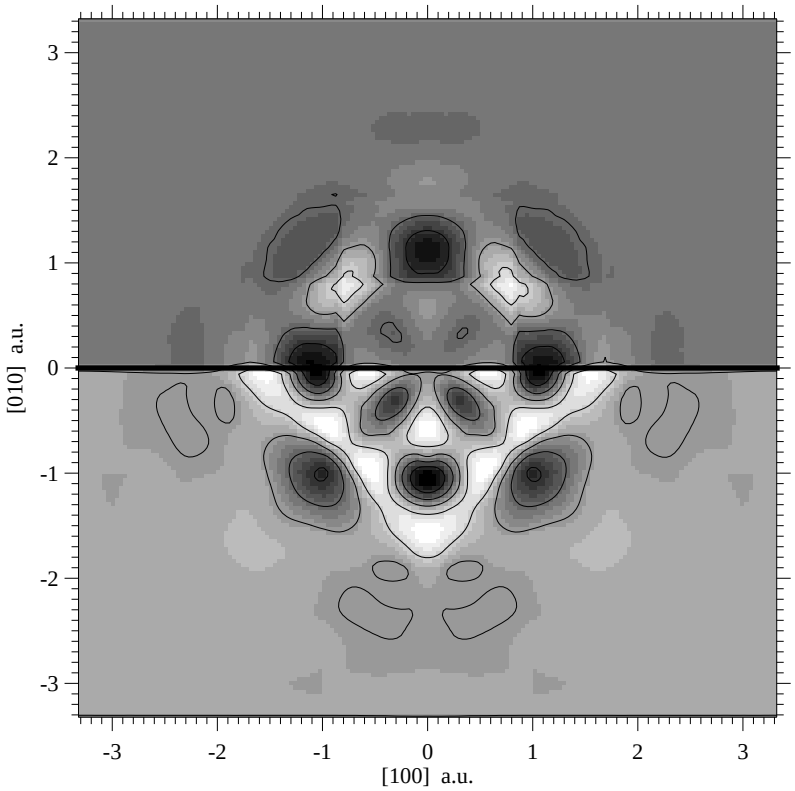

Figure 3. Radial anisotropy of the [001]-projected momentum density, coming from the experiment (top) and LMTO calculation (bottom).

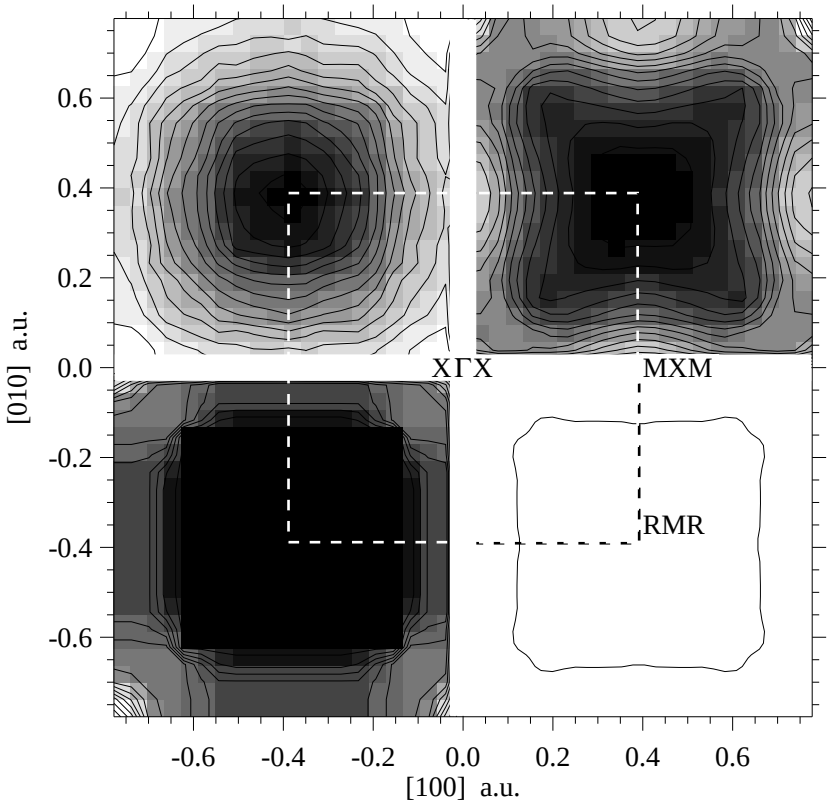

Figure 4. Top left: occupancy projected along [001], coming from the LCW-folded experimental spectra. Top right: LCW of calculated electron–positron momentum density. Bottom left: calculated electron occupancy. Bottom right: the 'woolsacks' FS, extracted from the experimental data by the zero-crossing procedure outlined in the main text. The Brillouin zone is marked by the dotted line, and the labels indicate the projected symmetry points.

The radial anisotropy of the data and LMTO calculation is plotted in figure 3. This is constructed by subtracting the radial average of the spectrum from the spectrum itself. The agreement between the experiment and theory is excellent. So as not to obscure any details, the theory has not been convoluted with the experimental resolution function. In complex, multi-band systems, it is often the case that the anisotropy is dominated by the fully occupied bands, rather than the valence bands, and as such does not reflect the topology of the underlying FS. An LMTO calculation of the anisotropy from just the oxygen sublattice shows that this provides the dominant contribution to the total anisotropy, i.e. as the states at the Fermi level are predominantly of Mn d character, the total anisotropy is not going to reflect the FS.

The LCW-folded data, together with the calculated electron, and electron–positron occupancies (projected down [001]) are shown in figure 4 as grayscale images, the white areas being the areas with the highest occupancy. Aside from some limited evidence for electron pockets at Γ, the dominant features in all are the woolsack hole pockets (see figure 2) centred on the *R* points of the BZ. These can be clearly identified in both the experimental and theoretical distributions, but owing to the smearing of the experimental resolution (and to some extent, perturbations introduced by the positron wave function), their precise size and shape is not clear. Additionally, the finite sampling in the calculations may slightly degrade their resolution.

Recent advances in the analysis methods for 2D-ACAR data have opened up the possibility for the extraction of extremely reliable and accurate information about the shape and size of the Fermi surface, even though the spectra are smeared with the experimental resolution and influenced by positron wave function effects. In most cases, a full 3D reconstruction is needed [10], and hence it is necessary to measure a series of projections along different directions. However, if the FS topology is relatively simple, as is the case here, this information can be gleaned from just one projection. This is because the hole cuboids of interest project onto themselves, and are not obscured by any other FS feature. Previously, it was proposed by Dugdale *et al* [19, 20] that it is possible to define the FS by a zero-crossing contour in a filtered distribution. The filtering method used there was based on maximum entropy, but band-pass filters were being simultaneously employed for a similar purpose [21]. More recently, these techniques were used to reveal the FS of yttrium, and extract quantitative information about a particular sheet [22]. In the bottom right of figure 4, this zero-crossing contour is plotted, and it is evident that it is very square in shape. (A similar procedure applied to the theoretical electron–positron distribution gave very similar results.) This supports the idea that this sheet of FS does indeed have the nesting and skipping properties referred to earlier. In addition, the size of the cube has been determined as $0.65 \pm 0.02 \times (2\pi/a)$. This compares reasonably with the value of $0.78 \times (2\pi/a)$ taken from the LMTO theory (and that of $0.81 \times (2\pi/a)$, found by Pickett and Singh [9]). The Γ-centred electron surface does not appear to be defined by this zero-contour. This could be because its shape is more spherical than the flat-sided hole cubes and hence does not generate as sharp an edge in the projection, thus not being as 'enhanced' by the band-pass filter.

In conclusion, we have measured the Fermi surface topology of $La_{0.7}Sr_{0.3}MnO_3$ using the 2D-ACAR technique. Our results agree well with the findings of our own band structure calculation and with those of others [8, 9]. In particular, using recently implemented methods for determining the FS, we have shown the existence of a cuboid hole FS sheet, centred on the *R* point of the Brillouin zone. The cuboid has been shown to have a side of $0.65 \pm 0.02 \times (2\pi/a)$, and to be sufficiently flat for the carrier 'skipping' and nesting described by Pickett and Singh [9] to be extremely favourable.

We are particularly indebted to Professor Tokura (JRCAT, Japan) for providing the sample. We would also like to acknowledge support from the Texas Advanced Research Program (Grant No 003656-142). One of us (SBD) would also like to thank the Lloyd's of London Tercentenary Foundation for the provision of his fellowship, and the EPSRC (UK) for other support.

References

[1] von Helmholt R M, Wecker J, Holzapfel B, Schultz L and Samwer K 1993 *Phys. Rev. Lett.* **71** 2331
[2] Jin S, Tiefel T H, McCormack M, Fastnacht R A, Ramesh R and Chen C H 1994 *Science* **264** 413
[3] Ramirez A P 1997 *J. Phys.: Condens. Matter* **9** 8171
[4] Venkatesan T, Rajeswari M, Dong Z W, Ogale S B and Ramesh R 1998 *Phil. Trans. R. Soc.* A **356** 1661
[5] Satpathy S, Popovic Z S and Vukajlovic F R 1996 *Phys. Rev. Lett.* **76** 960
Solovyev I, Hamada N and Terakura K 1996 *Phys. Rev. Lett.* **76** 4825
[6] Millis A J, Littlewood P B and Shraiman B I 1995 *Phys. Rev. Lett.* **75** 5144
Millis A J, Shraiman B I and Mueller R 1996 *Phys. Rev. Lett.* **77** 175
[7] Singh D J and Pickett W E 1998 *Phys. Rev.* B **57** 88
[8] Youn S J and Min B I 1998 *J. Korean Phys. Soc.* **32** 576
[9] Pickett W E and Singh D J 1997 *Phys. Rev.* B **55** R8642
[10] West R N 1995 *Proc. Int. School of Physics, 'Enrico Fermi'—Positron Spectroscopy of Solids* ed A Dupasquier and A P Mills Jr (Amsterdam: IOS Press)
[11] Jarlborg T and Singh A K 1987 *Phys. Rev.* B **36** 4660

[12] Lock D G, Crisp V H C and West R N 1973 *J. Phys. F: Met. Phys.* **3** 561
[13] Urushibara A, Moritomo Y, Arima T, Asamitsu A, Kido G and Tokura Y 1995 *Phys. Rev.* B **51** 14 103
[14] West R N, Mayers J and Walters P A 1981 *J. Phys. E: Sci. Instrum.* **14** 478
[15] Andersen O K 1975 *Phys. Rev.* B **12** 3060
Jarlborg T and Arbman G 1977 *J. Phys. F: Met. Phys.* **7** 1635
[16] Perdew J P 1985 *Phys. Rev. Lett.* **55** 1665
[17] Singh A K and Jarlborg T J. Phys. F: Met. Phys. **15** 727 (1985)
[18] Pickett W E, Krakauer H and Cohen R E 1990 *Physica* B **165 & 166** 1057
Krakauer H, Pickett W E and Cohen R E 1993 *Phys. Rev.* B **47** 1002
[19] Dugdale S B, Alam M A, Fretwell H M, Biasini M and Wilson D 1994 *J. Phys.:Condens. Matter* **6** L435
[20] Dugdale S B 1996 *PhD Thesis* University of Bristol, UK
[21] O'Brien K M, Brand M Z, Rayner S and West R N 1995 *J. Phys.: Condens. Matter* **7** 925
[22] Dugdale S B, Fretwell H M, Alam M A, Kontrym-Sznjad G, West R N and Badrzadeh S 1997 *Phys. Rev. Lett.* **79** 941